

PAPER • OPEN ACCESS

Hypoxia adapted relative biological effectiveness models for proton therapy: a simulation study

To cite this article: Guillermo Garrido-Hernandez *et al* 2022 *Biomed. Phys. Eng. Express* **8** 065026

View the [article online](#) for updates and enhancements.

You may also like

- [In-plane elastic properties of auxetic multilattices](#)
Igor E Berinskii
- [The effect of probiotics on digestive enzyme activity during larvae and juvenile stage of Yellow Fin Tuna \(*Thunnus albacares*\)](#)
Haryanti, Gunawan, A Setiadi et al.
- [CONSTRAINTS ON THE INITIAL-FINAL MASS RELATION FROM WIDE DOUBLE WHITE DWARFS](#)
Jeff J. Andrews, Marcel A. Agüeros, A. Gianninas et al.

Biomedical Physics & Engineering Express



PAPER

Hypoxia adapted relative biological effectiveness models for proton therapy: a simulation study

OPEN ACCESS

RECEIVED
27 May 2022

REVISED
29 September 2022

ACCEPTED FOR PUBLICATION
18 October 2022

PUBLISHED
4 November 2022

Original content from this work may be used under the terms of the [Creative Commons Attribution 4.0 licence](#).

Any further distribution of this work must maintain attribution to the author(s) and the title of the work, journal citation and DOI.



Guillermo Garrido-Hernandez¹ , Helge Henjum², Marte Kåstad Høiskar¹, Tordis Johnsen Dahle^{2,3}, Kathrine Røe Redalen¹ and Kristian Smeland Ytre-Hauge² 

¹ Department of Physics, Norwegian University of Science and Technology, Trondheim, Norway

² Department of Physics and Technology, University of Bergen, Bergen, Norway

³ Department of Oncology and Medical Physics, Haukeland University Hospital, Norway

E-mail: guillermo.g.hernandez@ntnu.no

Keywords: proton therapy, hypoxia, oxygen enhancement ratio, relative biological effectiveness, monte carlo

Supplementary material for this article is available [online](#)

Abstract

In proton therapy, a constant relative biological effectiveness (RBE) factor of 1.1 is applied although the RBE has been shown to depend on factors including the Linear Energy Transfer (LET). The biological effectiveness of radiotherapy has also been shown to depend on the level of oxygenation, quantified by the oxygen enhancement ratio (OER). To estimate the biological effectiveness across different levels of oxygenation the RBE-OER-weighted dose (ROWD) can be used. To investigate the consistency between different approaches to estimate ROWD, we implemented and compared OER models in a Monte Carlo (MC) simulation tool. Five OER models were explored: Wenzl and Wilkens 2011 (WEN), Tinganelli *et al* 2015 (TIN), Strigari *et al* 2018 (STR), Dahle *et al* 2020 (DAH) and Mein *et al* 2021 (MEI). OER calculations were combined with a proton RBE model and the microdosimetric kinetic model for ROWD calculations. ROWD and OER were studied for a water phantom scenario and a head and neck cancer case using hypoxia PET data for the OER calculation. The OER and ROWD estimates from the WEN, MEI and DAH showed good agreement while STR and TIN gave higher OER values and lower ROWD. The WEN, STR and DAH showed some degree of OER-LET dependency while this was negligible for the MEI and TIN models. The ROWD for all implemented models is reduced in hypoxic regions with an OER of 1.0–2.1 in the target volume. While some variations between the models were observed, all models display a large difference in the estimated dose from hypoxic and normoxic regions. This shows the potential to increase the dose or LET in hypoxic regions or reduce the dose to normoxic regions which again could lead to normal tissue sparing. With reliable hypoxia imaging, RBE-OER weighting could become a useful tool for proton therapy plan optimization.

1. Introduction

Tumor hypoxia (low oxygenation) is associated with radioresistance, potentially leading to treatment failure and poor disease survival [1, 2]. The increased radioresistance of hypoxic tumors is estimated by means of the oxygen enhancement ratio (OER), defined as the ratio of radiation doses in hypoxic (D_{hyp}) and fully oxygenated conditions (D_{norm}) that result in the same cell surviving fraction. The effects of hypoxia on photon radiation have been known for a long time, where the OER commonly is between 2 and

3 [3]. High linear energy transfer (LET) radiation, characteristic of heavy-ion radiotherapy, is little affected by hypoxia, resulting in an OER close to 1 [4]. With proton therapy, as a low to mid LET radiation type, the effect of hypoxia is intermediate, with typical OER values around 1.5–2.5 depending on the energy [2].

Proton and heavy-ion radiotherapy are more efficient than photon radiotherapy because they induce more complex, clustered DNA damage that is more difficult to repair. Radiation efficiency relative to photons is quantified by the relative biological

effectiveness (RBE) [5, 6]. The proton-RBE may be used to estimate the biological dose (D_{bio}) of a proton therapy plan. D_{bio} accounts for the different biological effect of protons compared to conventional photon radiation and is found by weighting the physical dose (D_{phys}) with the RBE, i.e., $D_{bio} = RBE \cdot D_{phys}$. Many RBE models have been proposed up to date [7], but in daily clinical practice the consensus is to adopt a 1.1 constant RBE. However, several studies have shown that the RBE is not constant and that it depends on factors such as the deposited physical dose, the radiation quality, and the irradiated tissue type [6–11]. Proton therapy plans may benefit from using a variable RBE and from accounting for the OER [11, 12].

Proton therapy plans can be adapted using the microdosimetric kinetic model (MKM), a model that can predict the RBE for heavy ions [10, 13, 14], and others are based on phenomenological models [7, 15]. These RBE models rely on experimental data such as the radiosensitivity parameters α and β from the linear quadratic (LQ) model. And with both, it is possible to perform a hypoxia adaptation to estimate and study the RBE-OER weighted dose (ROWD). Several models to adapt the RBE for hypoxia have been published for proton therapy [16–24], but how these models agree or differ in their predictions has not yet been studied. Therefore, before a potential hypoxia adaptation of clinical proton therapy plans, there is a need to investigate and compare the performance of the different models.

In this study, we aimed to implement and analyze different hypoxia adapting RBE models in order to compare the predicted OER and the resulting ROWD for proton therapy. Five published models that weight the RBE using the OER were implemented in the FLUKA Monte Carlo (MC) simulation framework. For each model, we simulated proton therapy plans both on a virtual water phantom and on a head and neck cancer (HNC) patient case where hypoxia was quantified by positron emission tomography (PET) imaging using a hypoxia tracer.

2. Materials and methods

2.1. Calculating the RBE for proton therapy

With the formalism presented by the LQ model [25], the RBE can be expressed as

$$RBE(D_p, \alpha_x, \beta_x, \alpha, \beta) = \frac{1}{D_p} \cdot \left(\sqrt{\left(\frac{\alpha_x}{2\beta_x}\right)^2 + \frac{\alpha D_p + \beta D_p^2}{\beta_x}} - \frac{\alpha_x}{2\beta_x} \right) \quad (1)$$

showing that the RBE depends on the proton physical dose (D_p) and the radiosensitivity parameters of the tissue, α , β , α_x and β_x [26, 27]. The α and β corresponds to the radiation sensitivity for protons and α_x and β_x to the sensitivity for photons, the reference radiation. Note that some of these models define the extreme values, achieving the parameters

RBE_{max} and RBE_{min} and rewrite equation (1) to calculate the RBE [7].

2.1.1. Rørvik RBE model (ROR)

ROR developed a proton-RBE model by defining the extreme RBE values, RBE_{max} and RBE_{min} , as the high and low dose limits. Resulting in $RBE_{max} = \alpha/\alpha_x$ and $RBE_{min} = \sqrt{\beta/\beta_x}$ [15]. When substituting these into equation (1) it becomes

$$RBE(D_p, \alpha_x/\beta_x, RBE_{max}, RBE_{min}) = \frac{1}{2D_p} \cdot \left(\sqrt{\left(\frac{\alpha_x}{\beta_x}\right)^2 + 4D_p \left(\frac{\alpha_x}{\beta_x}\right) RBE_{max} + 4D_p^2 RBE_{min}^2} - \frac{\alpha_x}{\beta_x} \right). \quad (2)$$

Furthermore, ROR includes a biological weighting function (BWF) based on phenomenological data from *in vitro* cell experiments to include a dependency in RBE_{max} on the full dose weighted LET spectrum. Finally, it assumes a constant $\beta = \beta_x$ that makes $RBE_{min} = 1$ [15]. Using these RBE_{max} and RBE_{min} in equation (2) the ROR-RBE is obtained.

2.1.2. Microdosimetric kinetic model (MKM)

The MKM can predict the RBE of heavy-ion (high-LET) radiation [10, 13, 28, 29]. It defines the number of lethal lesions produced in the cell nucleus averaged over a cell population to describe the surviving fraction S after cell irradiation as $\ln(S) = -(\alpha_0 + \beta z_{1D}^*) D_{phys} - \beta D_{phys}^2$ [14, 30, 31]. Making an analogy with LQ model, the MKM defines its radiosensitivity parameters $\alpha_{MKM} = (\alpha_0 + \beta z_{1D}^*)$ and $\beta_{MKM} = \beta$. Where α_0 and β are often taken as the reference photon α_x and β_x parameters [31–33] and z_{1D}^* is the saturation-corrected dose-mean specific energy from a single event [30, 33]. Substituting α_{MKM} and β_{MKM} for α and β in equation (1) the MKM-RBE is estimated.

2.2. OER models and RBE adaptation

Hypoxia can be quantified by the partial oxygen pressure (pO_2), expressed in % or in mmHg. Different approaches to calculate the OER from pO_2 have been proposed [16–24]. Generally, these models use experimental *in vitro* data from different cell lines under normoxic and hypoxic conditions to fit a reverse-sigmoid shaped curve describing the OER and pO_2 relationship through the Alper-Howard-Flanders formalism [3]. In general, the experimental data defined their normoxic data to correspond to 160 mmHg or 21% oxygenation. From how the fitted experimental data is used on the modeling and estimation of the OER, we see that the models follow two different methods.

The first methods is used by the adaptations proposed by Mein *et al* (MEI) [19] and Tinganelli *et al* (TIN) [18], who use published and in-house phenomenological data, respectively, to parameterize the OER

for photons (OER_{ph}) as a function of the pO_2 and then correct for high LET-particles using a radiation quality parameter, L . For these models, the resulting OER follows

$$OER(L, pO_2) = \frac{a \cdot OER_{ph}(pO_2) + L^\gamma}{a + L^\gamma} \quad (3)$$

where a and γ are parameters obtained from the numerical fit to the experimental data and OER_{ph} is described as

$$OER_{ph}(pO_2) = \frac{m \cdot K + pO_2}{K + pO_2} \quad (4)$$

where the m and K are constants obtained via a numerical fit to the experimental data [34, 35].

The second method is used on the OER models by Wenzl and Wilkens (WEN) [16], Dahle *et al* (DAH) [20] and Strigari *et al* (STR) [22], and it consists of adapting the LQ radiosensitivity parameters, $\alpha(L)$ and $\beta(L)$, to account for hypoxia. The modeled $\alpha(L, pO_2)$ and $\beta(L, pO_2)$ are then used to calculate the OER using equation (5) [16, 36], obtained after expanding iso-effective D_{hyp} and D_{norm} , and where p_{norm} is the partial oxygen pressure in normoxic conditions and S is the surviving fraction.

$$OER(L, pO_2) = \frac{\sqrt{\alpha^2(L, pO_2) - 4\beta(L, pO_2)\ln(S)} - \alpha(L, pO_2)}{\sqrt{\alpha^2(L, p_{norm}) - 4\beta(L, p_{norm})\ln(S)} - \alpha(L, p_{norm})} \cdot \frac{\beta(L, p_{norm})}{\beta(L, pO_2)} \quad (5)$$

The calculated OER, regardless of whether is directly modeled (first method) or calculated from the hypoxia adapted LQ parameters (second method), is then used together with the RBE to define the ROWD-factor, described in this study as $RO = RBE/OER$. This makes the ROWD-factor an RBE relative to photon radiation at normoxic conditions. The ROWD is then calculated as $ROWD = D_{phys} \cdot RO$ where D_{phys} is the total physical dose.

Adaptations that use the modeled OER using methods resulting in heavy, time-consuming numerical calculations [21, 23] and earlier versions of the studied OER models [17] were left out in this work. A summary of all the studied models can be found in table 1. The table shows that some models account for the oxygenation level by measuring the pO_2 in % and other models by using mmHg. However, the conversion from one unit to the other is trivial [37].

To account for oxygenation effects, OER models are used in combination with an RBE model. Particularly, the studied OER models could have been used together with a low/intermediate-LET RBE model or with an RBE model that considers high-LET radiation as well. At the time of coupling the OER models with an RBE model we followed the approach detailed in the models' original publications. Consequently, in the present

work, both WEN and DAH were used to adapt for hypoxia together with the variable RBE model by Rørvik *et al* (ROR) [15] and a constant RBE of 1.1 ($RBE_{1.1}$) (low/intermediate-LET RBE). The TIN, MEI, and STR models were combined with the RBE in the MKM framework (high-LET RBE).

2.2.1. Wenzl and Wilkens OER model (WEN)

WEN modeled the LQ parameters accounting for the LET and the pO_2 measured in mmHg, before adjusting the OER [16]. In this framework, the whole LET dependence is carried by α and β is LET independent. Following the Alper-Howard-Flanders relation [3], the Wenzl and Wilkens α and β parametrization follows:

$$\alpha(LET_d, pO_2) = \frac{(a_1 + a_2 \cdot LET_d) \cdot pO_2 + (a_3 + a_4 \cdot LET_d) \cdot K}{pO_2 + K} \quad (6)$$

and

$$\sqrt{\beta(pO_2)} = \frac{b_1 \cdot pO_2 + b_2 \cdot K}{pO_2 + K} \quad (7)$$

where $K = 3.0$ mmHg, LET_d is the dose-averaged linear energy transfer, $a_1 = 0.22 \text{ Gy}^{-1}$, $a_2 = 0.0024 \text{ } \mu\text{mGy}^{-1}\text{keV}^{-1}$, $a_3 = 0.05 \text{ Gy}^{-1}$, $a_4 = 0.0031 \text{ } \mu\text{mGy}^{-1}\text{keV}^{-1}$, $b_1 = 0.4 \text{ Gy}^{-1}$ and $b_2 = 0.015 \text{ Gy}^{-1}$ [16]. The WEN model used results from OER experiments for several cell lines (V79, HSG, HeLa, p388, FSa-II, R1, T1, L2, EMT6, SCC VII, NFSa, RAT1, and 9L), to find 10% cell survival for multiple radiation types (protons, deuterons, He-, C-, Ne- and Ar-ions) under normoxic and hypoxic conditions.

2.2.2. Dahle OER model (DAH)

The model by Dahle *et al* is based on the WEN model. The particularity of this model is that it only uses experimental proton data from several cell lines (V79, HSG, T1, HeLa, p388, and H₄) to parametrize the LQ-parameters following equations (6) and (7), resulting in $a_1 = 0.1 \text{ Gy}^{-1}$, $a_2 = 0.001 \text{ } \mu\text{mGy}^{-1}\text{keV}^{-1}$, $a_3 = 0.01 \text{ Gy}^{-1}$, $a_4 = 0.001 \text{ } \mu\text{mGy}^{-1}\text{keV}^{-1}$, $b_1 = 0.765 \text{ Gy}^{-1}$ and $b_2 = 0.237 \text{ Gy}^{-1}$ [20].

2.2.3. Mein OER model (MEI)

MEI modeled a parameter called the hypoxia reduction factor (HRF) that acts as the OER to account for hypoxia [19]. The HRF depends on the pO_2 in % and a dimensionless particle and energy dependent

Table 1. Summary of oxygen enhanced ratio (OER) models for particle therapy. MKM = microdosimetric kinetic model, HRF = hypoxia reduction factor, LET = linear energy transfer, pO_2 = partial oxygen pressure.

	Fitted data ^c			Modeled parameters ^d	Dependencies ^e	MKM adapting
	Cell lines	Particles	Survival fraction			
Wenzl and Wilkens (WEN) [16]	HSG V79 CHO others ^a	protons deuterons He-ions C-ions Ne-ions Ar-ions	0.1	α_{hyp} β_{hyp}	LET _d pO_2 [mmHg]	NO
Tinganelli et al (TIN) [18]	V79 CHO	x-rays C-ions N-ions O-ions Si-ions	0.1	OER_{ph} OER_{ion}	LET _d pO_2 [%]	YES
Dahle et al (DAH) [20]	HSG V79 others ^b	protons	0.1	α_{hyp} β_{hyp}	LET _d pO_2 [mmHg]	NO
Mein et al (MEI) [19]	V79	protons He-ions C-ions	0.1	HRF_{ph} HRF_{ion}	$(Z_{eff} / \beta_{ion})^2$ pO_2 [%]	YES
Strigari et al (STR) [22]	HSG V79 CHO	He-ions C-ions Ne-ions	0.1	$\alpha_{MKM-hyp}$ $\beta_{MKM-hyp}$	$\bar{z}_{1D} \bar{z}_{1Dn}$ pO_2 [mmHg]	YES

^a others: HeLa, p388, F5a-II, R1, T1, L2, EMT6, SCC VII, NFSa, RAT1, and 9L.

^b others: T1, HeLa, p388, and H₄.

^c Fitted data displays details on the irradiated cell lines, the type of radiation used to acquire the experimental data and the survival fraction of the irradiated cells.

^d Modeled parameters are obtained from the experimental data and are specific for each model.

^e Dependencies of the models are listed, as these may affect the OER adaptation ($\beta_{ion} = v/c$). Note that some of them imply a tissue type, particle type and/or particle energy dependence.

parameter, the radiation quality energy, $RQE = (Z_{eff} / \beta_{ion})^2$. Z_{eff} is the effective charge of the ionizing particle and $\beta_{ion} = v/c$, where v is the velocity of the particle and c the speed of light.

MEI first takes the photon OER modelling [34, 35] to introduce the photon HRF as:

$$HRF_{ph}(pO_2) = \frac{pO_2 + m \cdot K}{pO_2 + K}, \quad (8)$$

where $m = 2.94$ and $K = 0.129\%$.

Data from OER experiments for protons, alpha particles and carbon ions is used to perform a second parametrization to include the RQE dependence. HRF_{ion} , is then calculated as

$$HRF_{ion}(RQE, pO_2) = \frac{a \cdot HRF_{ph}(pO_2) + RQE^\gamma}{a + RQE^\gamma} \quad (9)$$

where $a = 2.988 \cdot 10^6$ and $\gamma = 2.169$ [19]. The HRF_{ion} from MEI is used as the OER, previously defined in equation (3).

MEI is based on *in vitro* experimental data from the V79 cell line irradiated with proton and higher-LET radiation data from heavier ions, and it was used to adapt the MKM, an RBE model for high-LET radiation.

2.2.4. Tinganelli OER model (TIN)

Similar to MEI, TIN parametrizes the OER using a two-step process to include the pO_2 in % and the LET_d [18], enabling adaptation also to heavy-ion RBE models, i.e., TIN can also be used to adapt the MKM.

First, the LET_d dependence is introduced in anoxic conditions, i.e., $pO_2 = 0\%$, and the OER is given by

$$OER(LET_d, 0\%) = \frac{LET_d^\gamma + M \cdot a}{a + LET_d^\gamma}, \quad (10)$$

where $M = 2.7$, $a = 8.27 \cdot 10^5$ (keV/μm)^γ and $\gamma = 3.0$. This fit was performed on V79 cell line data from an extensive dataset measured at NIRS and then adapted to the Chinese hamster ovary (CHO) cell line data set that was subject of their study [18].

In a second step, the pO_2 dependence is included resulting in

$$OER(LET_d, pO_2) = \frac{b \cdot m + pO_2}{b + pO_2}, \quad (11)$$

where $b = 0.25\%$ according to an x-ray data parametrization [38] and $m = OER(LET_d, 0\%)$ as described in equation (10) [19].

2.2.5. Strigari OER model (STR)

STR is intended to use with the MKM, and it considers the specificity of different ions, LET and tissue type

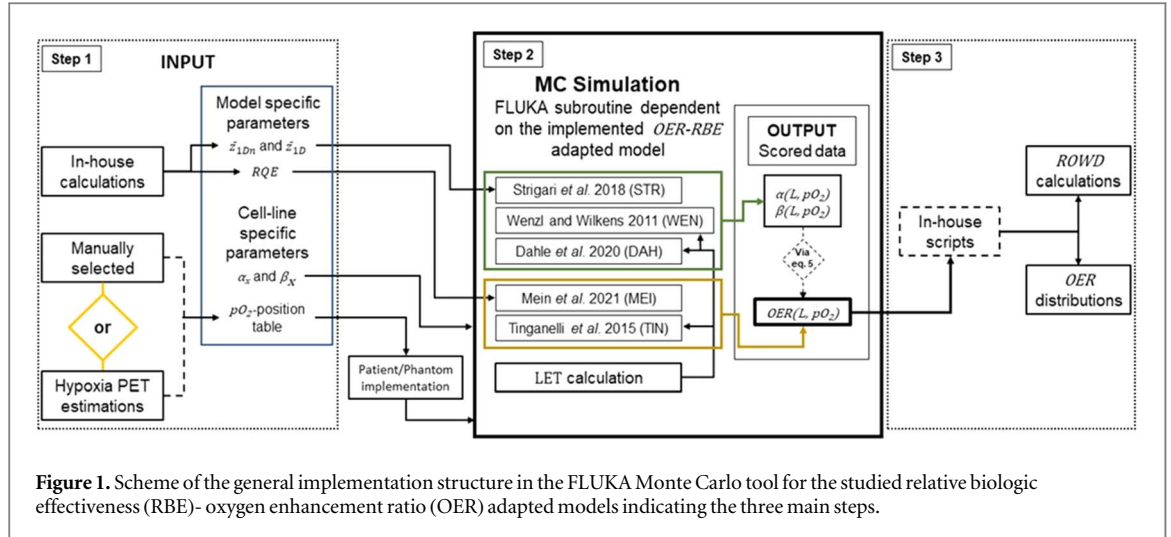


Figure 1. Scheme of the general implementation structure in the FLUKA Monte Carlo tool for the studied relative biologic effectiveness (RBE)-oxygen enhancement ratio (OER) adapted models indicating the three main steps.

[22]. STR models the α and β parameters from the MKM and defining $\alpha(pO_2)$ and $\beta(pO_2)$ as

$$\alpha(pO_2) = \frac{\alpha_{max} \cdot pO_2 + \alpha_{min} \cdot K}{pO_2 + K} \quad (12)$$

and

$$\sqrt{\beta(pO_2)} = \frac{\sqrt{\beta_{max}} \cdot pO_2 + \sqrt{\beta_{min}} \cdot K}{pO_2 + K}. \quad (13)$$

The α_{min} and β_{min} correspond to the LQ radiosensitivity parameters under extreme hypoxic conditions, with pO_2 close to 0 mmHg while α_{max} and β_{max} correspond to normoxic conditions. These parameters are evaluated accounting for the non-Poisson lethal event distributions for high-LET particles by multiplying α_{MKM} with a correction factor [13, 31], resulting in

$$\alpha = \frac{1 - \exp(-\alpha_{MKM} \bar{z}_{1Dn})}{\bar{z}_{1Dn}} \cdot \alpha_{MKM}, \quad (14)$$

where \bar{z}_{1Dn} is the dose-averaged specific energy in the nucleus and $\alpha_{MKM} = \alpha^0 + \beta^0 \bar{z}_{1D}$, where \bar{z}_{1D} is the dose-averaged specific energy in the domain and α^0 and β^0 the LQ radiosensitivity parameters used in the MKM. These parameters were fitted to experimental *in vitro* data for the HSG, V79 and CHO cell lines under normoxic and extreme hypoxic conditions to obtain the α_{max}^0 and α_{min}^0 parameters needed to solve equation (12).

To account for non-Poisson lethal event distributions for high-LET particles for β_{MKM} parameter they multiplied it by $(\alpha/\alpha_{MKM})^2$ resulting in

$$\beta = \left(\frac{\alpha}{\alpha_{MKM}} \right)^2 \cdot \beta_{MKM}, \quad (15)$$

where α is obtained from equation (14) and $\beta_{MKM} = \beta^0$. From equation (15) they obtain the β_{max}^0 and β_{min}^0 needed to solve equation (13). Note that equation (15) the same scaling between LQ-parameters in the MKM.

Details on the dose-averaged specific energies \bar{z}_{1Dn} and \bar{z}_{1D} are beyond the scope of this study, these can be found elsewhere [39, 40]. Their calculation was carried out as described by Kase *et al* 2008 [31], and for their implementation in FLUKA we followed the approach from Magro *et al* 2017 [33].

2.3. Monte Carlo implementation

We implemented these five OER models in the FLUKA MC tool [41] following three steps as indicated in figure 1:

1. Input data is created and organized into input tables that are read by FLUKA. These include the pO_2 -position table needed for hypoxia adaptations and the radiation quality parameter tables required for each model. Single-track dose-averaged specific energies or the RQE were calculated and given to FLUKA as \bar{z}_{1Dn} -energy, \bar{z}_{1D} -energy and RQE-energy tables. With an internal subroutine, FLUKA uses the proton energy recorded at each step of the Monte Carlo simulation to interpolate and use the corresponding radiation quality parameter on the corresponding voxel.
2. Based on the input data and the corresponding radiotherapy plan input file, FLUKA calculates the model parameters with a dedicated subroutine for each model. Depending on the model, FLUKA will calculate and score the $OER(L, pO_2)$. Note that for WEN, DAH and STR, the $OER(L, pO_2)$ is scored after estimating the $\alpha(L, pO_2)$ and $\beta(L, pO_2)$ parameters and using them into equation (5).
3. FLUKA output is studied with in-house Python scripts. The calculated and scored $OER(L, pO_2)$ is used together with the scored physical dose and the RBE specific α and β parameters to estimate the ROWD, create OER-maps, dose-volume histograms (DVHs) and assess the effects of hypoxia on the original proton plan.

2.4. Model simulations on a virtual water phantom and in a patient case

To study and evaluate the five OER models, MC simulations were performed using the in-house FLUKA based system for treatment plan recalculation [42] with standard FLUKA physics settings (PRECISION defaults, a delta-ray threshold of 10 keV and a logarithmic width of dp/dx momentum loss tabulated interval of 1.03, as recommended for particle therapy) and activating the modified RQMD (Relativistic Quantum Molecular Dynamics) for nucleus-nucleus interactions above 125 MeV per nucleon. Detailed explanations of the FLUKA recalculation tool are found in [20, 42]. Results on the LET_d , D_{phys} , αD_{phys} and $\sqrt{\beta} D_{phys}$ were scored using the FLUKA subroutine *fluscw* (FLUence Scoring Weight) and, the number of primaries simulated was chosen to achieve a voxel mean statistical uncertainty below 2% and a voxel maximum statistical uncertainty below 3% in the target.

To verify the model implementation in FLUKA and evaluate the OER, a first set of MC simulations recalculated a proton field irradiating a water phantom. The proton field implemented in FLUKA was optimized in an analytical TPS to deliver, in a virtual water phantom, a homogeneous D_{bio} of 2.0 Gy(RBE) in a $4 \times 4 \times 4$ cm³ volume that ranges from 8 cm to 12 cm depth in water using spread-out Bragg (SOBP) peaks. During the optimization process, the TPS used the constant $RBE_{1.1}$ for D_{bio} calculations. We first set a homogeneous pO_2 value for the whole water phantom and changed it in repeated simulations. The oxygenation (pO_2) levels ranged from fully hypoxic ($pO_2 = 0.0075$ mmHg or $pO_2 = 0.001\%$) to fully normoxic ($pO_2 = 160.0$ mmHg or $pO_2 = 21.13\%$) to score the corresponding $OER(L, pO_2)$ for different oxygenation levels. The results from these simulations were compared to the expected theoretical results from the implemented OER models.

Secondly, five 0.5 cm wide hypoxic layers were defined inside the virtual water phantom, perpendicular to the proton field incidence direction. The central layer corresponded to $pO_2 = 2.5$ mmHg (0.33%), the intermediate layer to $pO_2 = 10.0$ mmHg (1.32%) and the outer layer to $pO_2 = 20.0$ mmHg (2.63%). The rest of the water phantom was set to $pO_2 = 160.0$ mmHg (21.13%). These simulations enabled to mimic the clinical case in which the most severe hypoxia is found in the center of the target.

Finally, all implemented models were used to simulate a hypoxia-adapted proton therapy plan for a HNC case. Hypoxia imaging of the patient using [¹⁸F]-EF5 PET enabled quantification of oxygenation levels of the target volumes. The conversion from PET uptake to pO_2 values was calculated as previously published [20] where a threshold on the PET uptake data is implemented to keep pO_2 values from being

higher than 60 mmHg, this pO_2 value is generally taken as normoxic in the clinic [37, 43].

Since all studied OER models used data from the V79 cell line, all simulations were based on published data from the V79 cell line with normoxic LQ parameters of $\alpha_x = 0.147$ Gy⁻¹ and $\beta_x = 0.02$ Gy⁻² [21]. This was done to account for possible uncertainty effects in the results when simulating on a cell line not used when fitting the OER model parameters, and to minimize model differences caused by uncertainties arising from the use of different cell line data for different models.

2.5. Treatment plan

Treatment plans for both the virtual water phantom and patient case were created in the Eclipse (Varian Medical Systems, Palo Alto, CA, USA) treatment planning system (TPS), without accounting for hypoxia and were optimized for a constant RBE of 1.1.

For the HNC case, three proton fields were used to target the planning target volume (PTV). None of the three fields used a range shifter and were optimized with Eclipse TPS multifield optimization function to deliver a homogeneous $D_{RBE1.1}$ of 70 Gy(RBE) in 35 fractions to the PTV.

2.6. Model overview

Table 1 shows properties of the implemented OER models. Model differences arise from the mathematical modeling dependencies, the unit used for the pO_2 , the parameter used for radiation quality and the conditions under which the phenomenological data used by the OER models was obtained, i.e., the radiation type, the irradiated tissue type and the biological effect achieved, being this a survival fraction of 0.1 for all models. Regarding radiation type, WEN, TIN, and MEI were fit using data points from low and high LET radiation, DAH was fit using proton radiation data points, i.e., low LET, and STR was fit by only using data from high-LET radiation.

3. Results

3.1. OER study

All models show a clear increase in OER with decreasing pO_2 (figure 2). WEN, DAH and MEI agree well for clinically relevant pO_2 values on the studied patient case (~ 2.5 mmHg and above). For the same pO_2 values the maximum OER ranges between 1.4 and 2.1 for all models and, as expected, drops towards 1.0 as the pO_2 increases. The shape of the curve is different for STR, where the resulting OER diverges for low pO_2 values. In general, TIN and STR give higher OER than the other models, but while STR differs more at low pO_2 , the results are more similar to WEN, DAH and MEI at pO_2 above 8–9 mmHg than for TIN.

Figure 2 also shows higher OER with lower LET for all implemented OER models except TIN, that

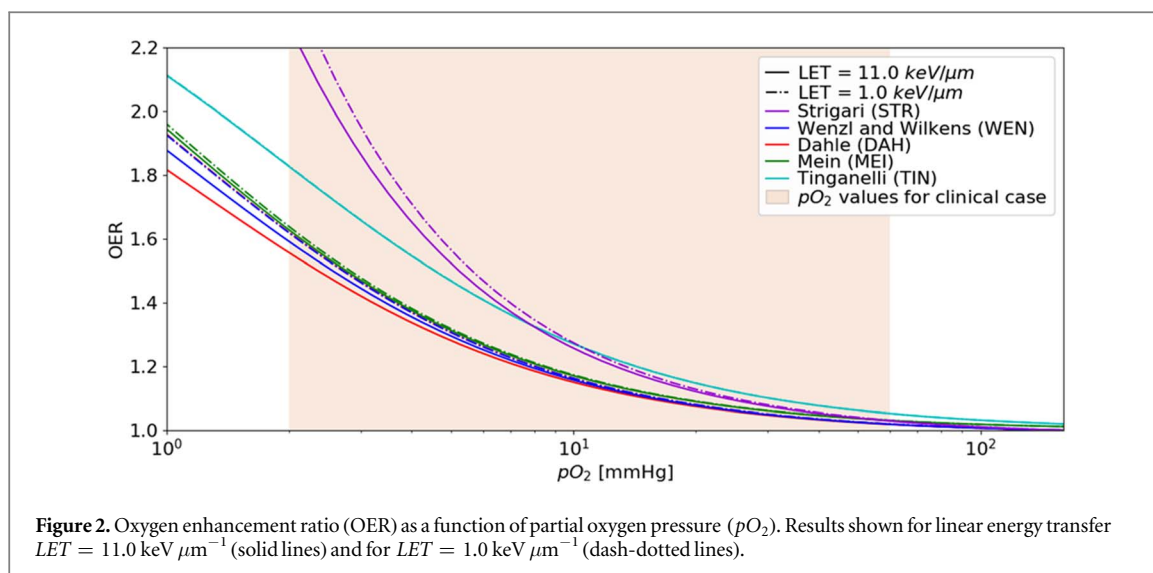


Figure 2. Oxygen enhancement ratio (OER) as a function of partial oxygen pressure (pO_2). Results shown for linear energy transfer $LET = 11.0 \text{ keV } \mu\text{m}^{-1}$ (solid lines) and for $LET = 1.0 \text{ keV } \mu\text{m}^{-1}$ (dash-dotted lines).

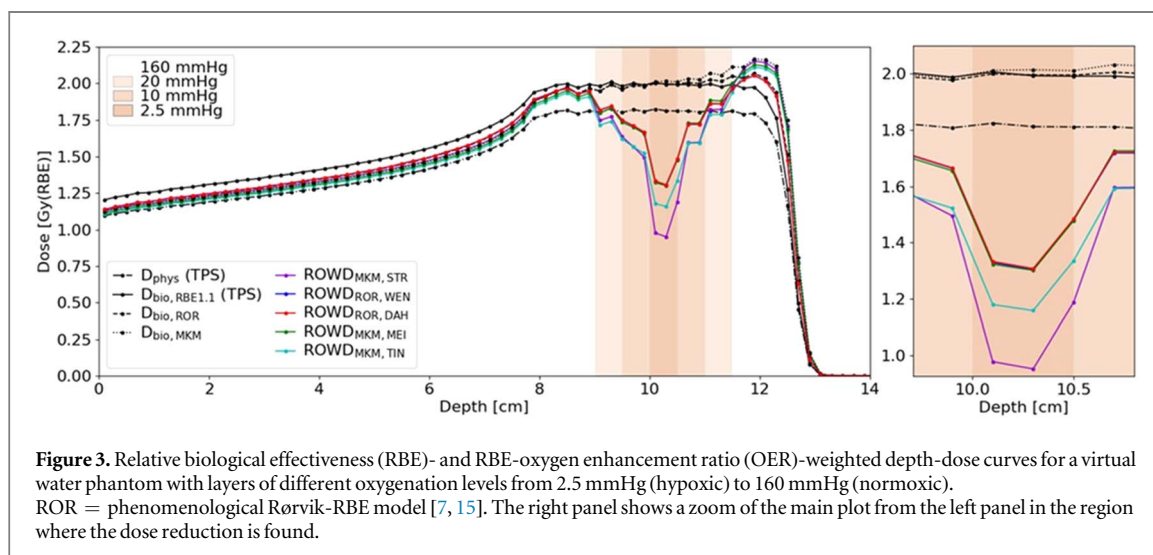


Figure 3. Relative biological effectiveness (RBE)- and RBE-oxygen enhancement ratio (OER)-weighted depth-dose curves for a virtual water phantom with layers of different oxygenation levels from 2.5 mmHg (hypoxic) to 160 mmHg (normoxic). ROR = phenomenological Rørvik-RBE model [7, 15]. The right panel shows a zoom of the main plot from the left panel in the region where the dose reduction is found.

exhibits no changes for the shown LET values of $1 \text{ keV } \mu\text{m}^{-1}$ and $11 \text{ keV } \mu\text{m}^{-1}$. However, WEN, DAH and STR have a stronger LET dependence than MEI.

How OER estimations from FLUKA fit to the theoretical results is shown in figure S1.

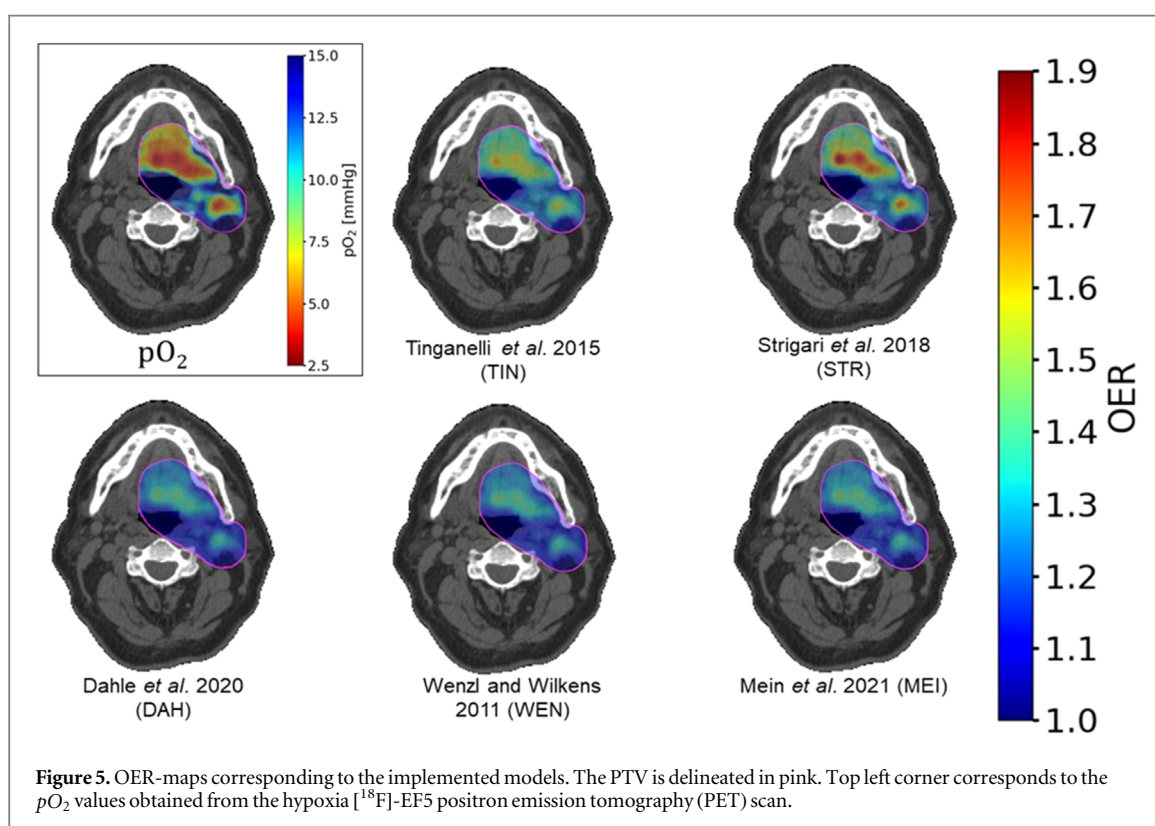
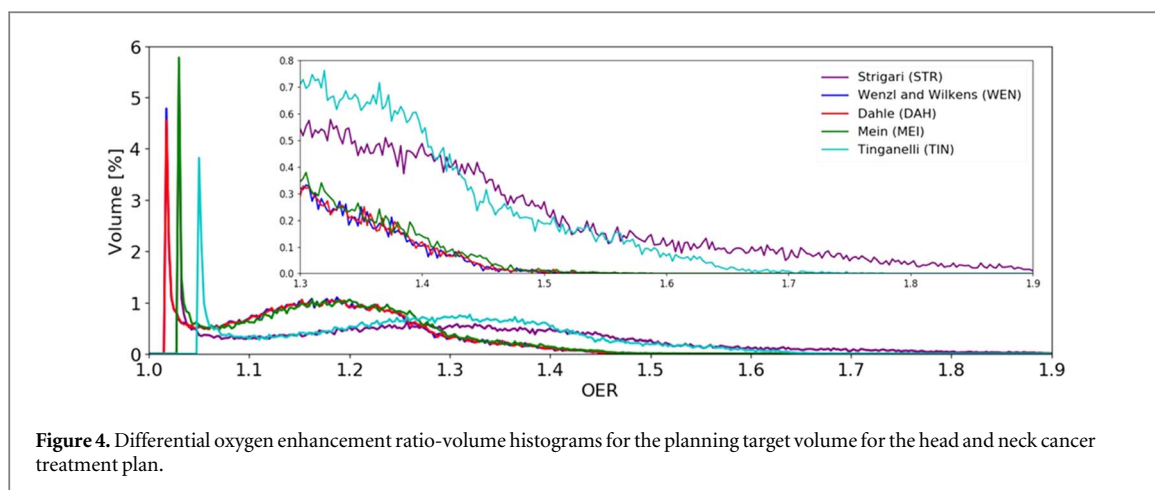
3.2. Oxygenation effect on the biological dose

The resulting ROWD from the different models for the water phantom simulations can be seen in figure 3. All hypoxia adapted RBE models show a dip in ROWD in the hypoxic layers placed between 8 cm and 12 cm depth. The dip in the 2.5 mmHg layer corresponds to a reduction in dose between 25% and 40% when comparing all ROWD results to the dose from normoxic RBE models ($D_{bio,RBE1.1}$, $D_{bio,ROR}$, and $D_{bio,MKM}$).

In the normoxic region ($pO_2 = 160 \text{ mmHg}$) all ROWDs approximated the D_{bio} estimated by the corresponding RBE model. In the first region with intermediate hypoxia ($pO_2 = 20 \text{ mmHg}$) the lowest ROWD is predicted by TIN and the highest by WEN, DAH and MEI, which estimate the highest ROWDs at

all hypoxic layers. In the second intermediate hypoxic region ($pO_2 = 10 \text{ mmHg}$) the ROWDs from STR and TIN cross, with STR being the model with the lowest results. In the most hypoxic layer ($pO_2 = 2.5 \text{ mmHg}$), the lowest ROWD is still estimated by STR. The ROWDs from the WEN and DAH models are indistinguishable at all depths and very similar to the ROWD from the MEI model in the hypoxic layers. The oxygen level at which results from TIN and STR cross is the same in both figures 2 and 3.

Differences in the ROWD within the same hypoxic regions for the same model are the result of inhomogeneities in the SOBP, which can be seen in the plotted D_{phys} , and the effects of averaging the ROWD values from voxels found on the boundary between hypoxic layers. As the voxel grid used in our simulations and the limits of the pO_2 layers do not match, the averaged value for the data points near these boundaries will be affected by the overlap of different pO_2 values within the same voxel. At the same time, D_{bio} results for the MKM model are higher than for the ROR model in the distal edge of the SOBP and slightly



lower in the plateau region. These differences are still noticeable after ROWD calculations.

3.3. Simulations on patient case

Figure 4 shows that for WEN, DAH, and MEI the volume percentage corresponding to the same OER is similar for the patient case, resulting in three similar differential OER-volume histograms. For TIN and STR the shapes are alike, with the differential OER-volume distribution slightly shifted towards higher OER values for STR, see zoom in plot in figure 4. The peaks at low OER correspond to the respective OER model predictions at $pO_2 = 60$ mmHg, the upper pO_2 limit set during the hypoxia PET data conversion.

The OER distributions for the patient case are also shown in figure 5, together with the LET and pO_2 distribution in the target. Similar OER maps are seen for WEN, DAH and MEI, while higher OER are observed for TIN and STR models. However, regions of OER variation were found to be consistent between all models.

The MC simulations show that the PTV received LET_d in the range of 1.1 – 5.3 $keV \mu m^{-1}$ with a mean value of 2.7 $keV \mu m^{-1}$. As for the pO_2 , it ranges between 2 mmHg and 60 mmHg in the PTV with a mean pO_2 of 9.75 mmHg.

Figure 6 shows ROWD volume histograms for each model. All models predict a ROWD lower than

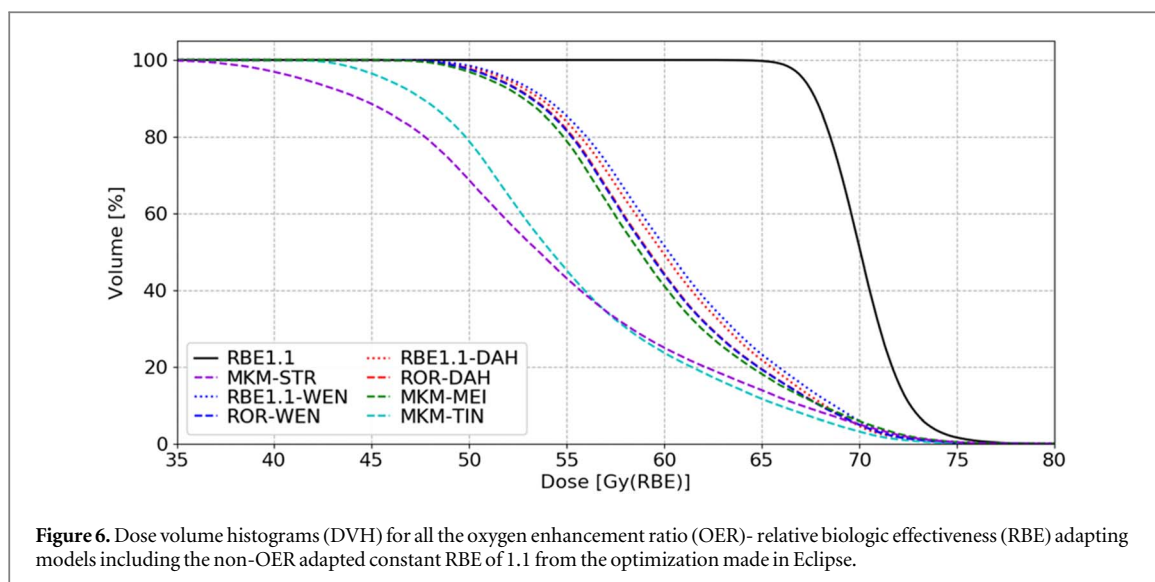


Table 2. ROWD received by 50% and 95% of the PTV ($ROWD_{50}$ and $ROWD_{95}$) and mean ROWD received by the PTV ($ROWD_{mean}$) according to the OER adaptations of the $RBE_{1.1}$, the ROR phenomenological RBE model, and the MKM.

	$ROWD_{50}$ [Gy(RBE)]	$ROWD_{95}$ [Gy(RBE)]	$ROWD_{mean}$ [Gy(RBE)]
$RBE_{1.1}$	70.0	67.0	70.1
Wenzl and Wilkens ($RBE_{1.1}$ -WEN) [16]	60.2	52.1	60.7
Wenzl and Wilkens (ROR-WEN) [16]	59.1	51.3	59.8
Tinganelli <i>et al</i> (MKM-TIN) [18]	54.2	45.7	55.4
Dahle <i>et al</i> ($RBE_{1.1}$ -DAH) [20]	59.9	51.9	60.3
Dahle <i>et al</i> (ROR-DAH) [20]	59.2	51.4	59.9
Mein <i>et al</i> (MKM-MEI) [19]	58.7	50.9	59.5
Strigari <i>et al</i> (MKM-STR) [22]	53.6	41.5	54.6

the normoxic $D_{RBE1.1}$ used in the plan optimization. The $ROWD_{50}$ ranged from 53.6 to 60.2 Gy(RBE), while the $D_{RBE1.1,50}$ is equal to 70.0 Gy(RBE). WEN and DAH give similar results when used to adapt the constant $RBE_{1.1}$ and the ROR phenomenological RBE. WEN and DAH show similar results as the MEI model. These three models predict a higher ROWD than STR and TIN. For WEN, DAH and MEI a $ROWD_{mean}$ between 58.7 and 60.2 Gy(RBE) is estimated, along with a $ROWD_{95}$ between 50.9 to 51.2 Gy(RBE). For TIN, $ROWD_{mean}$ is 54.2 Gy(RBE) and $ROWD_{95}$ is 45.7 Gy(RBE), while for STR $ROWD_{mean}$ equals 53.6 Gy(RBE) with a $ROWD_{95}$ of 41.5 Gy(RBE) respectively (table 2).

4. Discussion

In this study we implemented and compared previously published models that adapt the RBE in proton therapy for hypoxia through modelling of the OER. Using the FLUKA MC tool, we compared the OERs and resulting ROWDs predicted by each model. The evaluation was performed on a one field proton plan for a virtual water phantom with different hypoxia (pO_2) levels as well as on a three-field HNC patient case. When studying phenomenological models, we

must be aware that uncertainties in the experimental data affect the model parameters. Information about the precision of model parameters and their relationship with phenomenological uncertainties is not available in the literature. However, all studied models provide a methodology of estimating the OER and the OER-weighted dose to account for hypoxia. In the present work, we compare these models as they would be used in the clinic, where it is not a common practice to apply model uncertainties in the biological dose optimization process. We studied the effect of these models on the parameters from the V79 cell-line as this cell-line was included in all the model databases. This, together with enough primaries on the MC simulations to calculate physical quantities (voxel mean statistical uncertainty <2% and voxel maximum statistical uncertainty <3%), allows us to compare the outcome from the OER models as the impact of the assumptions made by the authors on the results instead of as the impact of the different uncertainties from the data on the results. A sensitivity study of the impact of uncertainties on dose estimates, as presented by Dahle *et al* [32], would be of high interest also for ROWD estimations.

As expected, OER-adapted RBE-models predict a lower biological dose absorption in hypoxic regions compared to RBE-models not adapted for hypoxia.

The observed sigmoid shape of the OER as a function of the pO_2 (figure 2) agrees with previous results [16–24]. All models show the same trend with increasing OER with reduced pO_2 , but while MEI, WEN and DAH agree very well across the range of clinically relevant hypoxia levels, TIN and STR predict higher OER over the whole pO_2 range. In particular, a higher OER for STR at low pO_2 is observed, which may be of clinical relevance.

OER variations for different LETs (figure 2) are also consistent with the expectations: we find higher OERs for lower LET values. This supports that high-LET radiation therapy is more efficient to treat aggressive hypoxic tumors. However, this LET difference is rather small for all models because the effect of the LET on the model equations is low for the studied pO_2 values and the limited range of LET present in proton therapy. Figures S2 and S3 show the extent of LET effects on extremely low, low and intermediate pO_2 concentrations on the OER and ROWD respectively. Yet, significant larger LET effects on the OER for WEN and DAH are captured when compared with MEI, STR and TIN. This might be explained by the phenomenological data used by the models: WEN and, in particular, DAH rely more on low- and intermediate-LET data compared to MEI, STR and TIN. DAH only used data from proton radiation, whereas STR used data from intermediate- (He-ions) and high-LET (C- and Ne-ions) radiation exclusively. WEN and MEI used data from low and high LET radiation throughout the OER modelling, whereas TIN modeled the photon OER and included the LET dependence considering only heavy-ion/high-LET data, which might explain why this dependence fades for TIN resulting in the same OER for different LETs. Even so, for the same LET, proton and heavy-ions do not result in the same radiation quality [44], making it not ideal to use an OER modeled with high-LET data for protons. Whether these models can be used to adapt for hypoxia high-LET radiation RBE models (like the MKM) has been explored or suggested in the literature can be seen in table 1. From figure 2 we suggest a two-group differentiation of the OER models, with WEN, DAH, and MEI in the first group and TIN and STR in the second group. This differentiation is independent of the two different methods in which the studied models estimate the OER. However, this two-group differentiation vanishes for extremely low pO_2 values (Figure S2) since the OER and its dependence with LET becomes specific for each model: WEN, DAH, MEI and TIN are seen to behave differently with increasing LET and STR results diverged and are one order of magnitude larger than for the other models for low LET. The latter could happen because the correction that STR makes to account for non-Poisson lethal event distributions for high-LET particles does not hold for proton LET, resulting in a divergence in the modeled OER for extremely low pO_2 values.

All adapted RBE models are LET dependent, which results in an increase of the biological dose towards the end of the SOBP when comparing to results with the RBE_{1,1} model (figure 3). After adapting these RBE models for hypoxia, all ROWDs reveal an increased biological dose at the end of the SOBP and a dose reduction in the hypoxic regions. The lowest pO_2 in the phantom simulation was 2.5 mmHg, which roughly corresponds to the lowest pO_2 in the patient case. Therefore, the approximated drop of 25% to 40% in the ROWD when compared to the D_{bio} should be expected in patient simulations when the LET of the incident protons and the pO_2 level selected as normoxic are the same in the phantom and the patient. These results support the same differentiation in two groups of models as the data from figure 2. This two-group model classification still holds when changing the reference α_x/β_x -ratio used on the adapted RBE models, (Figure S4). The WEN, DAH and MEI group shows a lower but still severe change of the absorbed dose estimated by the TPS and more homogeneous dose distributions than for the TIN and STR group. Still, all models exhibit a substantial ROWD decrease in specific tumor regions when accounting for the pO_2 . This would suggest increasing the dose to hypoxic regions during treatment plan optimization. Locating then the most radioresistant regions may allow to reduce the dose in the rest of the PTV, this would increase the complexity of the proton therapy plans in the clinic but overall reduce the dose to organs at risk (OARs). Ignoring the increased radioresistance of hypoxic tumor regions could potentially result in an ineffective treatment and poor patient outcome. Another solution would be to exploit the increased effectiveness of high-LET radiation on hypoxic tissue [45]. In this case, instead of boosting the dose on hypoxic tumor regions the LET could be increased. Our study indicates that, in the case of proton radiation, only a slight reduction in OER is obtained through LET increase (Figure S2). However, with the RBE increase achieved when increasing the LET, the ROWD could still be significantly augmented through the elevated LET (Figure S3).

As a final remark on the WEN, DAH and MEI models and calculations of the ROWD, we identified very similar results in spite of having adapted different RBE models (the MKM for MEI and ROR for WEN and DAH). Although unexpected, this is explained when looking at the differences between the normoxic $D_{bio,MKM}$ and $D_{bio,ROR}$ from 9 cm to 11.5 cm depth in figure 3. In this region of the SOBP we see how the normoxic ROR and MKM result in very similar D_{bio} . Therefore, any differences in the corresponding ROWD calculations would solely appear due to the OER adaptation. As seen in figure 2, there are only minor differences in the OER between WEN, DAH and MEI models for extremely low, low and intermediate oxygen levels. These two features put together

result in very similar ROWD calculations despite adapting different RBE models.

Since we have exclusively recalculated proton plans, and TIN and STR do not use proton data in their modelling, their results could be less reliable when compared with the WEN, DAH and MEI results. Among WEN, DAH, and MEI, we might select DAH as the most reliable model for proton plan recalculations since it is only based on proton data, but at the same time, this model is based on a smaller data set. However, the differences between these three models are so small that one could use other criteria to select which one to use, e.g., implementation complexity. However, we must consider that all these models carry an uncertainty that arises from the incertitude of the experimental data used for the modelling. Consequently, one might select the model after evaluating aspects such as the type of radiation, the energy and LET range, pO_2 range, pO_2 value set as normoxic condition, or the different cell-lines accounted for. For clinical use we must also acknowledge that the uncertainties will increase due to the lack of *in vivo* data and the uncertainties in the PET tracer uptake to pO_2 conversion method.

OER-maps (figure 5) go along with the estimated pO_2 distribution and the data from figures 2 and 3. As for the volume percentage peaks (figure 4) and their corresponding OER_{min} value, these appear due to the maximum pO_2 estimated from the hypoxia PET data. This value was set to 60 mmHg and was defined as the default normoxic pO_2 for PET uptake below a certain threshold [20] using as reference the normoxic pO_2 values in brain, muscle and fat (29.2 mmHg, 33.8 mmHg and 60.0 mmHg respectively) found in the literature [37, 43]. The model differences result in slightly different minimum OERs, between 1.01 and 1.05 depending on the model. This occurs because the cell data used in the models take 160 mmHg as the normoxic value. If the data used in the OER models took 60 mmHg as the normoxic value, matching the normoxic pO_2 in the clinical case, these peaks would appear at OER equal to 1. Consequently, when using any of these OER adaptations on clinical cases it should be considered to include a normalization step to ensure that we find an OER of 1 on the normoxic patient tissue, avoiding the calculation of an overdosage of these regions during a later optimization process. Only WEN and DAH comment on a normalization step for clinical recalculations. The effects of setting different pO_2 values as normoxic on the OER can be seen in figure S5. These normalization steps reduce the OER as we lower the reference pO_2 value for normoxic tissue. Therefore, this would reduce the depth of the dip of the ROWD in hypoxic regions shown on figure 3.

The differences in height of the volume percentage peaks that correspond to the OER_{min} are affected by the influence of the LET on each model: larger OER variations with the LET result in a lower volume with

OER_{min} . This argument is not valid for TIN, where the dispersion of low OER is a direct consequence of the rapid variation of the OER when increasing the pO_2 . The OER curve from TIN approaches 1.0 slower than the OER curves from the other models (figure 2), resulting in a larger variety of OER for high pO_2 values. Therefore, after a hypothetical normalization step to adapt the models to clinical cases, the volume percentage differences at OER equal to 1 would still be noticeable since it is affected by the dependence of the OER model with LET. Consequently, the proton-LET influence, although reduced, is noticeable in most of the studied OER models.

5. Conclusion

To summarize, we implemented a ROWD calculation in FLUKA MC using five different hypoxia adapted RBE models. Models were studied in terms of the consistency between their ROWD estimates to evaluate the impact of model assumptions, data selection and the potential for performing hypoxia adaptation of proton therapy plans. Results from simulations in both a virtual water phantom and a HNC case suggest a two-group classification of the models. The WEN, DAH and MEI models showed good agreement and more uniform dose distributions with lower OER values in low pO_2 regions when compared with the TIN and STR models. Application and comparison of the models indicated that the two latter models, primarily based on heavy ion data, potentially could overestimate the OER of protons at low pO_2 . Overall, all models display a large difference in the estimated dose from hypoxic and normoxic regions. This shows the potential to increase the dose or LET in hypoxic regions or reduce the dose to normoxic regions which again could lead to normal tissue sparing. The uncertainties in the OER models are however still largely unknown, but with quantification of uncertainties in the model parameters and reliable hypoxia imaging, RBE-OER weighting could become a useful tool for proton therapy plan optimization.

Acknowledgments

This work was supported by the Norwegian Research Council (project no. 299 651 and project no. 326 218) and the Trond Mohn Foundation (project no. TMS2019TMT08).


Data availability statement


All data that support the findings of this study are included within the article (and any supplementary files).

Ethics statement

This study was conducted in accordance with the Declaration of Helsinki. The patient data applied in this study was provided by Turku University Hospital and was used with permission from this facility. All patient material was anonymized, and the patient data from Turku University Hospital were part of a study registered at ClinTrials.Gov under No. NCT 01 774 760.

ORCID iDs

Guillermo Garrido-Hernandez  <https://orcid.org/0000-0002-4986-0154>

Kristian Smeland Ytre-Hauge  <https://orcid.org/0000-0002-3597-1611>

References

- [1] Brown J 2000 Exploiting tumour hypoxia in cancer treatment: mechanisms and therapeutic strategies *Mol Med Today* **6** 157–62
- [2] Gray L H, Conger A D, Ebert M, Hornsey S and Scott O C 1953 The concentration of oxygen dissolved in tissues at the time of irradiation as a factor in radiotherapy *Br. J. Radiol.* **26** 638–48
- [3] Alper T and Howard-Flanders P 1956 Role of oxygen in modifying the radiosensitivity of *E. coli* *B Nature* **178** 978–9
- [4] Nakano T et al 2006 Carbon beam therapy overcomes the radiation resistance of uterine cervical cancer originating from hypoxia *Clin. Cancer Res.* **12** 2185–90
- [5] Paganetti H, Niemierko A, Ancukiewicz M, Gerweck L E, Goitein M, Loeffler J S et al 2002 Relative biological effectiveness (RBE) values for proton beam therapy *Int. J. Radiat. Oncol. Biol. Phys.* **53** 407–21
- [6] Paganetti H 2014 Relative biological effectiveness (RBE) values for proton beam therapy. Variations as a function of biological endpoint, dose, and linear energy transfer *Phys. Med. Biol.* **59** R419–72
- [7] Rørvik E et al 2018 Exploration and application of phenomenological RBE models for proton therapy *Phys. Med. Biol.* **63** 185013
- [8] Belli M et al 2000 Inactivation of human normal and tumour cell irradiated with low energy protons *Int. J. Radiat. Biol.* **76** 831–9
- [9] Mohan R, Peeler C R, Guan F, Bronk L, Cao W and Grosshans D R 2017 Radiobiological issues in proton therapy *Acta Oncol.* **56** 1367–73
- [10] Hawkins R B 1994 A statistical theory of cell killing by radiation of varying linear energy transfer *Radiat. Res.* **140** 366–74
- [11] Carabe A, Moteabbed M, Depauw N, Schuemann J and Paganetti H 2012 Range uncertainty in proton therapy due to variable biological effectiveness *Phys. Med. Biol.* **57** 1159–72
- [12] Paganetti H et al 2019 Report of the AAPM TG-256 on the relative biological effectiveness of proton beams in radiation therapy *Med. Phys.* **46** e53–78
- [13] Hawkins R B 2003 A microdosimetric-kinetic model for the effect of non-poisson distribution of lethal lesions on the variation of RBE with LET *Radiat. Res.* **160** 61–9
- [14] Inaniwa T et al 2010 Treatment planning for a scanned carbon beam with a modified microdosimetric kinetic model *Phys. Med. Biol.* **55** 6721–37
- [15] Rørvik E, Thrørnqvist S, Stokkegåv C H, Dahle T J, Fjæra L F and Ytre-Hauge K S 2017 A phenomenological biological dose model for proton therapy based on linear energy transfer spectra *Med. Phys.* **44** 2584–94
- [16] Wenzl T and Wilkens J J 2011 Modelling of the oxygen enhancement ration for ion beam radiation therapy *Phys. Med. Biol.* **56** 3251–68
- [17] Scifoni E, Tinganelli W, Weyrather W K, Durante M, Maier A and Krämet M 2013 Including oxygen enhancement ration in ion beam treatment planning: model implementation and experimental verification *Phys. Med. Biol.* **58** 3871–95
- [18] Tinganelli W et al 2015 Kill-painting of hypoxic tumours in charged particle therapy *Sci Rep.* **5** 17016
- [19] Mein S et al 2021 Spot-scanning hadron arc (SHArc) therapy: a study with light and heavy Ions *Adv Radiat Oncol* **6** 100661
- [20] Dahle T J et al 2020 The FLUKA Monte Carlo code coupled with an OER model for biologically weighted dose calculations in proton therapy of hypoxic tumors *Phys Med* **76** 166–72
- [21] Bopp C, Hirayama R, Inaniwa T, Kitagawa A, Matsufuji N and Noda K 2016 Adaptation of the microdosimetric kinetic model to hypoxia *Phys. Med. Biol.* **61** 7586
- [22] Strigari L, Torriani F, Manganaro L, Inaniwa T, Dalmasso F, Cirio R et al 2018 Tumour control in ion beam radiotherapy with different ions in the presence of hypoxia: an oxygen enhancement ratio model based on the microdosimetric kinetic model *Phys. Med. Biol.* **63** 065012
- [23] Antonovic L, Lindblom E, Dasu A, Bassler N, Furusawa Y and Toma-Dasu L 2014 Clinical oxygen enhancement ratio of tumors in carbon ion radiotherapy: the influence of local oxygenation changes *J. Radiat. Res.* **55** 902–11
- [24] Grimes R D 2020 Estimation of the oxygen enhancement ratio for charged particle radiation *Phys. Med. Biol.* **65** 15NT01
- [25] McMahon S J 2019 The linear quadratic model: usage, interpretation and challenges *Phys. Med. Biol.* **64** 01TR01
- [26] Wilkens J J and Oelfke U 2004 A phenomenological model for the relative biological effectiveness in therapeutic proton beams *Phys. Med. Biol.* **49** 2811–25
- [27] Wedenberg M, Lind B K and Hårdemark B 2013 A model for the relative biological effectiveness of protons: the tissue specific parameter α/β of photons is a predictor for the sensitivity to LET changes *Acta Oncol.* **52** 580–8
- [28] Hawkins R B 1996 A microdosimetric-kinetic model of cell death from exposure to ionizing radiation of any LET, with experimental and clinical applications *Int. J. Radiat. Biol.* **69** 739–55
- [29] Hawkins R B 1998 A microdosimetric-kinetic theory of the dependence of the RBE for cell death on LET *Med. Phys.* **25** 1157–70
- [30] Kase Y et al 2006 Microdosimetric measurements and estimation of human cell survival for heavy-ion beams *Radiat. Res.* **166** 629–38
- [31] Kase Y, Kanai T, Matsufuji N, Furukawa T, Elsässer T and Scholz M 2008 Biophysical calculation of cell survival probabilities using amorphous track structure models for heavy-ion irradiation *Phys. Med. Biol.* **53** 37–59
- [32] Dahle T J, Magro G, Ytre-Hauge K S, Stokkegåv C H, Choi K and Mairani A 2018 Sensitivity study of the microdosimetric kinetic model parameters for carbon ion radiotherapy *Phys. Med. Biol.* **63** 225016
- [33] Magro G et al 2017 The FLUKA Monte Carlo code coupled with the NIRS approach for clinical dose calculations in carbon ion therapy *Phys. Med. Biol.* **62** 3814–27
- [34] Mairani A et al 2013 A Monte Carlo-based treatment planning tool for proton therapy *Phys. Med. Biol.* **58** 2471–90
- [35] Liew H et al 2019 Modeling of the effect of hypoxia and DNA repair inhibition on cell survival after photon irradiation *Int J Mol* **20** 6054
- [36] Wenzl T and Wilkens J J 2011 Theoretical analysis of the dose dependence of the oxygen enhancement ratio and its relevance for clinical applications *Radiat Oncol* **6** 171
- [37] Carreau A, Hafny-Rahbi B E, Matejuk A, Grillon C and Kieda C 2011 Why is the partial oxygen pressure of human tissues a crucial parameter? Small molecules and hypoxia *J. Cell. Mol. Med.* **15** 1239–53
- [38] Carlson D J, Stewart R D and Semenenko V A 2006 Effects of oxygen on intrinsic radiation sensitivity: A test of the relationship between aerobic and hypoxic linear-quadratic (LQ) model parameters *Med. Phys.* **33** 3105–15

- [39] Chatterjee A and Schaefer H J 1976 Microdosimetric structure of heavy ion tracks in tissue *Radiat. Environ. Biophys.* **13** 215–27
- [40] Kiefer J and Straaten H 1986 A model of ion track structure based on classical collision dynamics *Phys. Med. Biol.* **31** 1201–9
- [41] Battistoni G *et al* 2016 The FLUKA Code: An Accurate Simulation Tool for Particle Therapy *Front Oncol* **6** 116
- [42] Fjæra L F *et al* 2017 Linear energy transfer distributions in the brainstem depending on tumour location in intensity-modulated proton therapy of paediatric cancer *Acta Oncol.* **56** 763–8
- [43] Netzer N, Gatterer H, Faulhaber M, Burtscher M, Pramsohler S and Pesta D 2015 Hypoxia, Oxidative Stress and Fat *Biomolecules* **5** 1143–50
- [44] Friedrich T, Durante M and Scholz M 2013 Particle species dependence of cell survival RBE: Evident and not negligible *Acta Oncol.* **52** 589–603
- [45] Bassler N *et al* 2014 LET-painting increases tumour control probability in hypoxic tumours *Acta Oncol.* **53** 25–32